Sensor signal processing

A New Approach for Real-Time Center-of-Pressure Correction in Pressure Sensitive Mats Using Feedforward Neural Networks

Sergio Domínguez Gimeno[1*], Raul Igual Catalán[2], Carlos Medrano Sánchez[1], Inmaculada Plaza García[1**], Javier Martínez Cesteros[3], and Marco Pasetti[4*]

[1]*Engineering and Communications, Universidad de Zaragoza, 44003 Teruel, Spain*
[2]*Department of Electric Engineering, Universidad de Zaragoza, 44003 Teruel, Spain*
[3]*Department of Computer Science, Systems Engineering, Universidad de Zaragoza, 44003 Teruel, Spain*
[4]*Department of Information Engineering, Universita degli Studi di Brescia, 25123 Brescia, Italy*
[*]*Member, IEEE*
[**]*Senior Member, IEEE*

Manuscript received 14 February 2025; revised 28 March 2025 and 21 July 2025; accepted 18 August 2025. Date of publication 20 August 2025; date of current version 29 August 2025.

Abstract—Center-of-pressure (CoP) is a good clinical indicator in balance tests and fall-risk assessment. It can be detected using pressure sensitive mats (PSMs), which are affordable. However, these can suffer from certain nonidealities, such as hysteresis and creep. These effects have been assessed in literature. However, proposed algorithms have low computation speed and are complex. In this work, a completely new approach based on feedforward neural networks (FFNNs) is proposed with the goal of correcting the CoP given by PSMs, allowing real-time correction. Its performance is compared in terms of error and computation times with a state-of-the-art model, which corrects for hysteresis and creep in the PSM. Results show that FFNN can correct for the CoP measurements, providing a good accuracy-speed balance.

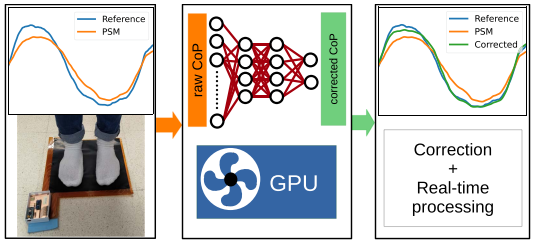

Index Terms—Sensor signal processing, center-of-pressure (CoP), feedforward neural network (FFN), piezoresistive sensor array, pressure sensitive mat (PSM), sensor signal processsing.

I. INTRODUCTION

The center-of-pressure (CoP) has been widely studied as a good indicator for balance assessment and fall-risk detection among elder people [1]. One way to measure the CoP position is to ask the person to stand on both feet on some measuring device. These can be force platforms (FPs) [2] or pressure sensitive mats (PSMs) [3]. PSMs have several advantages over FPs. They are more flexible, easier to transport, lighter, thinner, more customizable and affordable, etc. PSMs typically use a microcontroller to control sensor readout and process the data in real time. PSMs can be manufactured using accessible piezoresistive materials, such as Velostat [3], whose resistance changes upon the exertion of pressure. A 16 × 16 PSM is formed by 16 rows and columns of sensors, which provide 256 conductance values. From these arrays of conductances, the CoP coordinates can be obtained using (1). In this equation, G(i, j) is the value of the conductance of the (i, j) element, and (x_i, y_j) is its position in the PSM. It gives the CoP coordinates $\mathbf{U}$ of the person standing on it. Equation (1) would represent the actual CoP position if the conductance of each element was proportional to the pressure applied on it [3]. However, these affordable piezoresistive materials exhibit several nonidealities, such as hysteresis and creep [4], [5]. These effects do not deteriorate PSMs in the long term, but have shown to worsen CoP detection. In [3], a model that compensates for creep and hysteresis taxel-by-taxel in 16 × 16 PSMs was developed. CoP readouts are improved with this model. This correction is slow because it compensates for these effects in each taxel at a time

$$U(x, y) = \frac{\sum_{i,j} G(i, j) \cdot (x_i, y_j)}{\sum_{i,j} G(i, j)}. \tag{1}$$

Neural networks (NNs) have been previously applied for CoP detection in various ways: Liu et al. [6] developed a convolutional NN for CoP and ground reaction forces estimation during stair walking using FPs and a 3-D motion capture system. In [7], a multilayer perceptron is used to predict the age and fall probability of elder people taking several CoP indicators as inputs. In the field of wearable sensors, in [8], both the CoP and ground reaction force are estimated by an artificial NN, giving as inputs, such as the force of the force-sensitive resistor (FSR) sensors, as well as their first and second derivatives. Choi et al. [9] use commercially available sensorized insoles to predict CoP using both an FFNN and a long-short term memory NN. In [10], the position of a set of commercial sensors attached to the insole is optimized to obtain a better CoP estimation.

FPs are expensive commercial devices that show negligible errors in CoP detection. FSR sensors can be a good choice for low-density PSM, as their hysteresis or creep effects are low. However, they are expensive for higher sensor densities. Little work has been done on the correction of PSM nonidealities using NNs. In this work, a completely new approach is proposed: FFNNs are used to correct the output given by a PSM, which suffers from several nonidealities, using the CoP obtained by the proportional model as input [see (1)]. To do this, N samples of $\mathbf{U}$ are fed into the network. Its output $\hat{O}$ is a corrected

Corresponding author: Sergio Domínguez Gimeno (e-mail: sdominguezg@unizar.es).
Associate Editor: F. Falcone.
Digital Object Identifier 10.1109/LSENS.2025.3601010

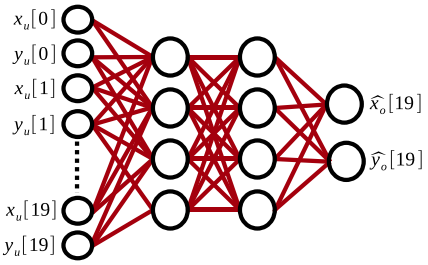

Fig. 1. Proposed approach (N = 20). The input is CoP samples obtained with the proportional model **U**. The output is the corrected CoP at k = 19; $\hat{O}$ [19].

CoP, closer to that given by, for example, an FP. This method is computationally faster and memory efficient, making it more suitable for embedding in microcontrollers (typically used in PSMs) than other approaches, such as [3]. These features are of interest in applications that require real-time CoP correction, such as long-term ergonomics studies, or in monitoring activities of daily life where a lot of data need to be processed. To assess the method's feasibility, it is compared with an optimized creep–hysteresis model proposed in [3]. This study shows that FFNNs provide similar accuracy results, but are much faster. FFNNs were selected because they are easy to set up and train with small datasets. They can capture temporal dynamics with a simple structure, improving interpretability in the CoP measurement context.

The rest of this letter is organized as follows. Section II presents the approach proposed in this letter. Section III introduces the experiments performed and the NN design. Section IV shows the results of this work. Finally, Section V concludes this letter.

II. PROPOSED APPROACH

Let **U** be the CoP signal obtained by assuming that the pressure–conductance relationship in the piezoresistive material is proportional [3], using (1). This is the proportional CoP model. Let **O** be the CoP signal provided by a reference device, such as an FP. Each **U** and **O** sample has two coordinates: $U[k] = (x_u[k], y_u[k])$ and $O[k] = (x_o[k], y_o[k])$. The FFNN receives N samples of **U** as an input, that is, the vector (U[k], U[k-1],..., U[k-N+1]), for k ≥ N-1. U[k] is the most recent sample. The FFNN predicts the current sample of the corrected CoP $\hat{O}[k]$. This approach is schematized in Fig. 1.

The number of CoP samples in the NN input is chosen as N = 20 from experience, as it gives good accuracy results. These range from the current sample U[k] to U[k-19]. To the best of the authors' knowledge, this approach is novel in the field of CoP correction using FFNNs. The idea of storing several signal samples is that the network can learn the trend of the signal at recent instants and correct for any temporal effects, similar to a filter.

The main advantages of this approach are its memory efficiency and computational speed. As the FFNN only needs 2 N CoP samples, only 2 N values need to be stored in memory. For a 16 × 16 PSM, 256 N values would be necessary in similar conditions [3]. An increase in computational speed can be expected for the same reason: the FFNN processes less samples than methods that consider all the sensors in the PSM. Moreover, the speed of this method is independent of the PSM size, as it uses a CoP signal as input. In addition, FFNNs can be easily parallelized and computed in GPUs, which also increases processing speed.

(a) (b) (c)

Fig. 2. Experimental setup. (a) Volunteer on the PSM and the FP. (b) Reference FP. (c) Top view of the plain PSM with data acquisition system.

III. MATERIALS AND METHODS

A. Instruments

The method has been tested in three different PSMs, each one having a different sensor structure. These are the same mats used in [3]. The three PSMs are 16 × 16, which means that they provide a 16 × 16 conductance array. The differences between them lie in the type of electrode and the position of the piezoresistive materialas follows.

1) *Interdigital PSM:* The two sensor electrodes are on the same layer of the printed circuit board (PCB) and the piezoresistive sheet lies on them. It has been manufactured by the researchers and use Velostat.
2) *Plain PSM:* It has two conductive layers, between which the piezoresistive material lies, forming a sandwich structure.
3) *Commercial PSM:* Manufactured by *Sensing Tex* [11]. In its documentation, it is said that it is based on textile technology and electronic ink.

All three PSMs have a scanning frequency of 100 Hz. An off-the-shelf FP manufactured by Pasco, model PS-2141 PASPORT, is used as the reference device [12]. Thus, **O** for training and evaluation are obtained with this device. As mentioned before, this device's nonidealities can be considered negligible compared to those of the PSMs.

B. Data Recording and Preprocessing

Data were obtained from 15 human volunteers,[1] (11 males and four females) with the following characteristics: height 1.75 ± 0.1 m, weight 67.7 ± 15.0 kg, foot length 25.5 ± 1.7 cm, age 26.1± 8.2 years. These volunteers performed three exercises while standing on the PSMs [see Fig. 2(a)]: stand on the mat with the right foot while keeping in balance, the same exercise with the left foot, and, finally, performing circular movements with their body with both feet on the PSM. These three exercises were performed for 30 s. At the same time, the FP [see Fig. 2(b)] placed under the PSM [see Fig. 2(c)] recorded **O**. All experiments were conducted in a laboratory environment under the same conditions: floor supporting base, room temperature and humidity, etc. Data were obtained and processed in the same way and conditions as in [3]. Data were collected separately for the three PSMs. Then, data were proportionally scaled between [−1, 1], and the average value of both **U** and **O** are removed, as it is not relevant in balance assessment applications [1].

Then, data are arranged to apply the proposed approach. Since each PSM is sampled at 100 Hz, a 30-s signal consists of approximately 3000

[1]Consent was obtained from all volunteers and approval of all ethical, and experimental procedures and protocols was granted by the corresponding ethics committee: Comité de Ética de la Investigación de Aragón.

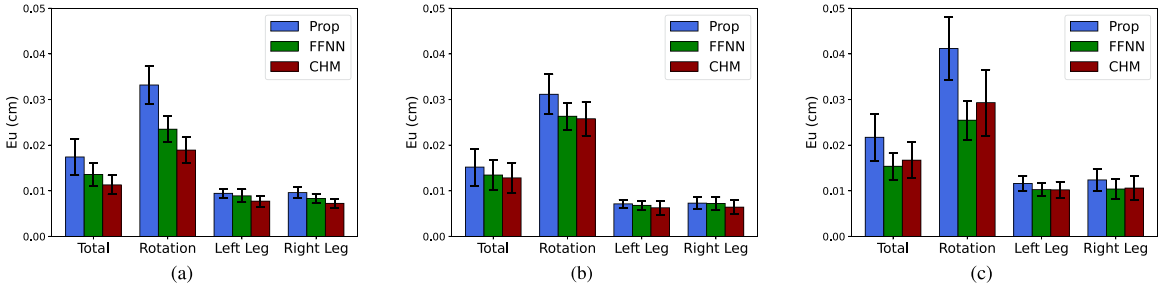

Fig. 3. Eu in cm and confidence intervals (confidence intervals (CI), 95%) for the proportional model (blue), the CHM (red), and FFNN (green) for each PSM. (a) Interdigital PSM. (b) Plain PSM. (c) Commercial PSM. Tests performed on the six subjects not used for training. Large CIs reflect intersubject variability. The variability between single-leg and rotation experiments is reflected in the "total" CIs.

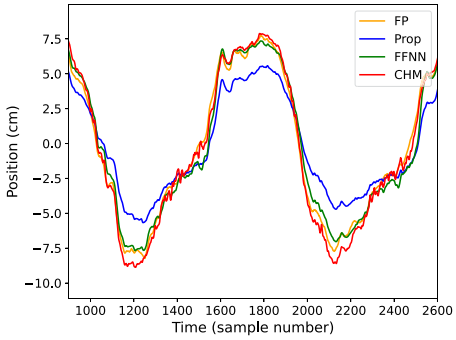

Fig. 4. Visual comparison of four CoP signals for the *x*-axis of a rotation experiment on the interdigital PSM. CoP signals are provided by the FP and all models, including the proportional (Prop, in blue).

samples. Each training sample consists of N = 20 CoP samples is as follows (as explained in Section II): the first training sample is the vector (U[19],...,U[0]), the second one is the vector (U[20],...,U[1]), and the last one is (U[3000],...,U[2981]). The output of sample (U[19],...,U[0]) is $\hat{O}$ [19] (see Fig. 1). The input can be seen as a shift register of N samples. Thus, 2982 training samples can be obtained from each 30 s signal. As each volunteer performs three experiments, 8946 samples are obtained per volunteer and per PSM. To ensure the generalizability of the proposed FFNNs, data from only three volunteers were used for training and validation. Two volunteers were used for training and the remaining one for validation, repeating this process three times per PSM (alternating the validation volunteer). Thus, three FFNNs per PSM were obtained. Then, samples from the remaining 12 volunteers, 107 352 samples (not involved in the training/validation process) were used for testing.

C. FFNN Design

The type of NN used in this work is FFNN, with fully connected layers. The structure chosen after a process of trial and error was (40, 60, 110, 20, and 2). Both input and output shapes match the sizes of the input and output samples. A network with fewer layers is faster than other networks with the same number of trainable parameters but more layers. With this number of parameters and the amount of training data, overfitting can be expected, so regularization has been applied to prevent it [13]. In this application, sigmoid-type activation functions are more appropriate than linear activations (such as rectified linear unit (ReLU)), because it presents bounded data [14]: the physical limits of the PSM. Thus, a hyperbolic tangent function has been used in all layers of all FFNNs [9].

This approach was implemented in Python (Keras-Tensorflow) on a PC with an AMD Ryzen 5 5600 G CPU (3.90 GHz), NVIDIA RTX 3050 GPU, 32 GB RAM, OS Windows 10 64-bit. The FFNNs were trained/tested on the GPU. All source codes are freely available under the gnu general public license (GPL) license in the GitLab repository [15].

D. FFNN Training and Validation

Training is performed using Adam optimizer with mean squared error (mse) loss function for 1000 epochs, and batch size is 4. This optimizer showed good overall performance in existing literature on CoP and NNs [6], [8], [10], [16]. A batch size of 4 was used as it showed low validation error values and because small batch sizes have the potential to have better generalization capability [14]. The process stops automatically if the mse in the validation set does not improve for 150 epochs in a row. Learning rate is set to 5e-6, and it is multiplied by 0.85 if the mse value does not improve for 25 consecutive epochs. During the training process, the model is saved if it improves the mse in the validation set.

E. Model Optimization

Model optimization was performed through structured parameter pruning [17]. One FFNN was trained for each PSM. It was observed that most of the weights of the original structure (40, 60, 110, 20, and 2) had values close to zero, which indicates that they do not perform any significant CoP correction. To optimize the number of neurons of each layer, the importance of each neuron can be measured by checking its L1-norm [17]. If the norm is under a threshold, then the neuron is discarded. The thresholds studied were 5e-5, 0.5, 0.7, 0.9, and 1.0, and those that minimized the error for the validation subject were taken as follows: 0.5 for the interdigital and plain PSMs, and 0.7 for the commercial PSM. This led to optimized structures for each PSM as: (40, 17, 15, 13, and 2), (40, 21, 18, 13, and 2), and (40, 14, 17, 12, and 2) for the interdigital, plain, and commercial PSMs, respectively. This results in lighter models with highly similar accuracy.

IV. RESULTS AND DISCUSSION

A. FFNN Performance in CoP Correction

In this section, the ability of the FFNN to correct for CoP measurements is assessed. To this end, two figures of merit have been used: the lock-step Euclidean distance between trajectories, Eu [3], and the percentage deviation. On the one hand, Eu is obtained for the proposed FFNNs. It is compared to the Eu of both the proportional

model and the creep–hysteresis model presented in [3] (from now on, CHM), which was also fitted using CoP data. On the other hand, point-to-point distances between FP coordinates and PSM coordinates are also calculated and expressed as a percentage deviation: % dev = 100*$\bar{d}$ (FP, M)/$\bar{d}$ (FP, 0), where $\bar{d}$ (FP, M) is the average distance between the points of the FP and PSM paths and $\bar{d}$ (FP,0) is the mean radius of the FP path. The points of the PSM paths are obtained using the FFNNs, the proportional model and the creep-hysteresis model (CHM) (as for Eu). This metric provides a relative error with respect to the amplitude of the movement.

As a result of this analysis, Fig. 3 represents the Eu for the proposed FFNN method, the proportional model, and the CHM. FFNNs improve the proportional model in all experiments and PSMs. In the rotation experiments, the improvement is great, but in single-leg experiments the improvement is not so large. However, in a one-to-one comparison, FFNNs outperform the proportional model in 55 out of the 72 single-leg experiments performed. Comparing to the CHM, the FFNN model shows similar levels of average error than the CHM, performing slightly worse in interdigital and plain PSMs, but improving in the commercial PSM (see Fig. 3). In a one-to-one comparison, the FFNN model improves the CHM in 36 out of 108 total experiments performed Fig. 4 shows the CoPs provided by the FP, and the three models: proportional, the FFNN, and CHM.

Concerning % dev, the values for the single-leg experiments were 40.7%, 46.1%, and 37.7% for the FFNNs, the proportional model, and the CHM, respectively. The values for the rotation experiments were 16.7%, 25.0%, and 16.5% for the FFNNs, the proportional model, and the CHM, respectively. This shows that all methods proportionally correct rotation experiments to a greater extent than single-leg experiments.

B. Computation Times

The computation time for both the FFNN and the CHM has been measured for a 30-s signal. The signal is processed and the average time is obtained. In the case of the FFNN, the average computation time is 3 s for all PSMs. The CHM proposed in [3] takes an average time of 22.1 s for all PSMs. This represents a processing frequency of 1000 samples/s for the FFNN and 137.5 samples/s for the CHM. It can be seen that the proposed approach greatly outperforms CHM in terms of speed. This is because it does not follow a taxel-by-taxel approach. Thus, it represents promising capabilities for real-time CoP correction.

V. CONCLUSION

In this work, FFNNs have been used to correct the CoP measurements from different PSMs in order to obtain accurate values. Compared to complex taxel-by-taxel models, FFNNs have a similar performance in terms of error, but with a higher computational speed. Processing frequency has been increased by a factor of 7.3, ensuring real-time CoP correction. Other types of NNs could be tested in the future for the same problem, although FFNNs have proven to be an effective, simple, and computationally efficient solution to correct CoP measurements in PSMs.

ACKNOWLEDGMENT

This work was supported in part by Departamento de Empleo, Ciencia y Universidades del Gobierno de Aragón under Grant T49_23R, in part by MCIN/AEI/10.13039/501100011033 under Grant PID21-125091OB-I00, in part by "ERDF A way of making Europe," in part by the Spanish Ministerio de Ciencia, Innovacion y Universidades under Grant PID21-125091OB-I00, in part by "Proyecto estratégico C077/23 del Instituto Nacional de Ciberseguridad (Spain)," in part by the Spanish Ministerio de Ciencia, Innovacion y Universidades under Grant PID21-125091OB-I00, and in part by Unizar, Ibercaja, CAI under Grant IT 1/24.

REFERENCES

[1] F. Quijoux et al., "Center of pressure displacement characteristics differentiate fall risk in older people: A systematic review with meta-analysis," *Ageing Res. Rev.*, vol. 62, 2020, Art. no. 101117.

[2] M. Piirtola and P. Era, "Force platform measurements as predictors of falls among older people–A review," *Gerontology*, vol. 52, no. 1, pp. 1–16, 2006.

[3] S. Domıńguez-Gimeno, C. Medrano-Sánchez, R. Igual-Catalán, and I. Plaza-Garcıá, "Optimized creep-hysteresis model to improve center-of-pressure detection in pressure sensitive mats," *IEEE Sensors J.*, vol. 25, no. 9, pp. 15295–15306, May 2025, doi: 10.1109/JSEN.2025.3550826.

[4] A. Arndt, "Correction for sensor creep in the evaluation of long-term plantar pressure data," *J. Biomech.*, vol. 36, no. 12, pp. 1813–1817, 2003. [Online]. Available: https://www.sciencedirect.com/science/article/pii/S002192900300229X

[5] S. Nizami, M. Cohen-McFarlane, J. R. Green, and R. Goubran, "Comparing metrological properties of pressure-sensitive mats for continuous patient monitoring," in *Proc. 2017 IEEE Sensors Appl. Symp.*, 2017, pp. 1–6.

[6] D. Liu, Y. Ma, J. Wang, M. Hou, and C. Zhang, "Convolutional neural network based ground reaction forces and center of pressure estimation during stair walking using multi-level kinematics," *Expert Syst. Appl.*, vol. 243, 2024, Art. no. 122868. [Online]. Available: https://www.sciencedirect.com/science/article/pii/S0957417423033705

[7] G. Shan, D. Daniels, and R. Gu, "Artificial neural networks and center-of-pressure modeling: A practical method for sensorimotor-degradation assessment," *J. Aging Phys. Activity*, vol. 12, no. 1, pp. 75–89, 2004.

[8] H. S. Choi, C. H. Lee, M. Shim, J. I. Han, and Y. S. Baek, "Design of an artificial neural network algorithm for a low-cost insole sensor to estimate the ground reaction force (GRF) and calibrate the center of pressure (CoP)," *Sensors*, vol. 18, no. 12, 2018, Art. no. 4349.

[9] A. Choi, H. Jung, K. Y. Lee, S. Lee, and J. H. Mun, "Machine learning approach to predict center of pressure trajectories in a complete gait cycle: A feedforward neural network vs. LSTM network," *Med. Biol. Eng. Comput.*, vol. 57, pp. 2693–2703, 2019.

[10] C.-W. Lin, S.-J. Ruan, W.-C. Hsu, Y.-W. Tu, and S.-L. Han, "Optimizing the sensor placement for foot plantar center of pressure without prior knowledge using deep reinforcement learning," *Sensors*, vol. 20, no. 19, 2020, Art. no. 5588. [Online]. Available: https://www.mdpi.com/1424-8220/20/19/5588

[11] Sensing Tex, "Pressure Mat Dev Kit 2.0," 2024. [Online]. Available: https://sensingtex.com/product/pressure-mat-dev-kit-2-0/

[12] PASCO, "Official website of PASCO," 2024. [Online]. Available: https://www.pasco.com/products/sensors/force/ps-2141

[13] Z. Farhadi, H. Bevrani, and M.-R. Feizi-Derakhshi, "Combining regularization and dropout techniques for deep convolutional neural network," in *Proc. 2022 Glob. Energy Conf.*, 2022, pp. 335–339.

[14] A. Géron, *Hands-On Machine Learning With Scikit-Learn, Keras, and TensorFlow*, 2nd ed. Sebastopol, CA, USA: O'Reilly Media, 2019.

[15] S. Dominguez-Gimeno and C. Medrano-Sanchez, "FFNN-CoP repository," (n.d.). [Online]. Available: https://gitlab.com/ctmedra1/ffnn_cop/-/releases

[16] D. P. Kingma and J. Ba, "Adam: A method for stochastic optimization," in *Proc. 3rd Int. Conf. Learn. Representations (ICLR)*, Banff, 14-16, April 2014.

[17] H. Li, A. Kadav, I. Durdanovic, H. Samet, and H. P. Graf, "Pruning filters for efficient convnets," in *Proc. Int. Conf. Learn. Representations*, 2017. [Online]. Available: https://openreview.net/forum?id=rJqFGTslg